

**MASARYK
UNIVERSITY**

FACULTY OF SCIENCE

**Diagnostics of High Power Impulse
Magnetron Sputtering Discharge**

Habilitation Thesis

JAROSLAV HNILICA

Department of Physical Electronics

Brno, 2023

MUNI
SCI

Bibliographic record

Author: Jaroslav Hnilica
Masaryk University
Faculty of Science
Department of Physical Electronics

Title of Thesis: Diagnostics of High Power Impulse Magnetron
Sputtering Discharge

Academic Year: 2022/2023

Number of Pages: 45

Keywords: magnetron, sputtering, HiPIMS, plasma diagnostics, optical emission spectroscopy, fast camera, strip probe, laser induced fluorescence

Abstract

The presented habilitation thesis called *Diagnostics of High Power Impulse Magnetron Sputtering Discharge* summarizes and comments on the results obtained during my work at the Department of Physical Electronics at the Faculty of Science of the Masaryk University together with the results attained in collaboration with colleagues from Academy of Sciences of the Czech Republic in Prague, University of Liverpool, Paris-Saclay University, National Institute for Optoelectronics in Bucharest and University of Mons. Eight papers showing a view on recent observation of the self-organization phenomenon in High Power Impulse Magnetron Sputtering discharge and spatial and temporal particle density evolution in the sputtering system were chosen to be presented in this work.

Acknowledgements

First, I would like to express my gratitude to my wife, Michaela, for her help and support, without which none of this would be possible. A special thanks are dedicated to my family and friends.

I would like to thank all my colleagues, present and past, local as well as from abroad.

Contents

List of commented publications	7
Introduction	9
1 Spokes in High Power Impulse Magnetron Sputtering	11
1.1 Introduction	11
1.2 The link between the oscillations of voltage and current induced by spokes	12
1.3 Study of spoke properties in broad range of experimental conditions	15
1.4 Spoke splitting and merging observed by high-speed camera and strip probes	18
1.5 In-depth investigation of spoke configuration	20
1.6 Conclusion	23
2 Dynamics of sputtered particles in HiPIMS	24
2.1 Introduction	24
2.2 Optical diagnostics for characterization of sputtering process	25
2.3 Diagnostics of standard and multi-pulse HiPIMS discharge	27
2.4 Spatial and temporal density evolution determined by LIF and AAS measurements	31
2.5 Conclusion	36
Bibliography	37
Author's publications not discussed in this work	42

List of commented publications

I have chosen eight research articles related to the spokes and dynamics of sputtered particles in HiPIMS discharge as a part of my thesis. The publications listed below are not ordered by publication date but according to the topic and as they appear within the following text. They are denoted as “AP,” which stands for annotated papers. My contribution to these articles is summarised in the following tables, with special attention to the experimental work, supervision of students, manuscript preparation, and research direction.

AP1 KLEIN, Peter; **HNILICA, Jaroslav**; HUBIČKA, Zdeněk; ČADA, Martin; ŠLAPANSKÁ, Marta; ZEMÁNEK, Miroslav; VAŠINA, Petr. Cathode voltage and discharge current oscillations in HiPIMS. *Plasma Sources Sci. Technol.* 2017, 26, 055015.

Experimental work	Supervision	Manuscript	Research direction
30%	50%	35%	15%

AP2 **HNILICA, Jaroslav**; KLEIN, Peter; ŠLAPANSKÁ, Marta; FEKETE, Matej; VAŠINA, Petr. Effect of magnetic field on spoke behaviour in HiPIMS plasma. *J. Phys. D: Appl. Phys.* 2018, 51, 095204.

Experimental work	Supervision	Manuscript	Research direction
25%	100%	50%	90%

AP3 KLEIN, Peter; LOCKWOOD ESTRIN, Francis; **HNILICA, Jaroslav**; VAŠINA, Petr; BRADLEY, James W. Simultaneous electrical and optical study of spoke rotation, merging and splitting in HiPIMS plasma. *Plasma Sources Sci. Technol.* 2017, 50, 015209.

Experimental work	Supervision	Manuscript	Research direction
30%	50%	25%	10%

AP4 KLEIN, Peter; **HNILICA, Jaroslav**; ZEMÁNEK, Miroslav; BRADLEY, James W; VAŠINA, Petr. The statistics of spoke configurations in high-power impulse magnetron sputtering discharges. *J. Phys. D: Appl. Phys.* 2019, 52, 125201.

LIST OF COMMENTED PUBLICATIONS

Experimental work	Supervision	Manuscript	Research direction
35%	50%	30%	20%

AP5 VAŠINA, Petr; FEKETE, Matej; **HNILICA, Jaroslav**; KLEIN, Peter; DOSOUDILOVÁ, Lenka; DVOŘÁK, Pavel; NAVRÁTIL, Zdeněk. Determination of titanium atom and ion densities in sputter deposition plasmas by optical emission spectroscopy. *Plasma Sources Sci. Technol.* 2015, 24, 065022.

Experimental work	Supervision	Manuscript	Research direction
10%	20%	25%	-

AP6 FEKETE, Matej; **HNILICA, Jaroslav**; VITELARU, Catalin; MINEA, Tiberiu; VAŠINA, Petr. Ti atom and Ti ion number density evolution in standard and multi-pulse HiPIMS. *J. Phys. D: Appl. Phys.* 2017, 45, 055201.

Experimental work	Supervision	Manuscript)	Research direction
35%	50%	30%	25%

AP7 **HNILICA, Jaroslav**; KLEIN, Peter; VAŠINA, Petr; SNYDERS, Rony; BRITUN, Nikolay. Revisiting particle dynamics in HiPIMS discharges. I. General effects. *J. Appl. Phys.* 2020, 128, 043303.

Experimental work	Supervision	Manuscript	Research direction
50%	-	40%	90%

AP8 **HNILICA, Jaroslav**; KLEIN, Peter; VAŠINA, Petr; SNYDERS, Rony; BRITUN, Nikolay. Revisiting particle dynamics in HiPIMS discharges. II. Plasma pulse effects. *J. Appl. Phys.* 2020, 128, 043304.

Experimental work	Supervision	Manuscript	Research direction
50%	-	40%	90%

Introduction

The presented habilitation thesis called *Diagnostics of High Power Impulse Magnetron Sputtering Discharge* summarizes and comments on the results obtained during my work at the Department of Physical Electronics at the Faculty of Science of Masaryk University. A significant part of the results was also attained in co-operation with colleagues from the Czech Republic and abroad, namely from Belgium, France, Romania, and United Kingdom. These works focus on non-intrusive spectroscopic discharge characterization techniques. In-situ non-intrusive discharge diagnostics is more favorable for precise and explicit discharge characterization as the plasma remains unperturbed in this case. I have participated in all the work presented in these studies, focusing on designing the experiments, methodology, investigation, and sputtered process description.

The presented work is divided into two chapters. The first chapter deals with plasma self-organization in High Power Impulse Magnetron Sputtering discharge. In 2012, three independent groups, all using fast imaging techniques, have simultaneously reported on plasma self-organization in this type of discharge. They observed that plasma is not homogeneously distributed over the target under certain experimental conditions, but it is localized into zones with enhanced ionization. Additionally, they discovered that these ionization zones rotate in the $\mathbf{E} \times \mathbf{B}$ direction above the racetrack area of the cathode (the racetrack being the area on the target with the highest erosion induced by the sputtering) with velocities of several km/s. Similar to moving regions of enhanced ionization observed in Hall thrusters called *spokes*; the ionization zones are now also called spokes in the magnetron sputtering community.

The second chapter is dedicated to determining the absolute number density of sputtered species in the discharge, one of the most crucial plasma diagnostics tasks. Such knowledge is necessary, especially the time- and space-resolved dynamics of the sputtered species in the ground state, to understand the plasma kinetics and chemistry. The absolute particle density could be used as input data to model the discharge processes. Moreover, the particle fluxes in the discharge, which are essential for the thin film growth process, can

be estimated by knowing the sputtered species density and velocity. The number densities of sputtered species are determined using the effective branching fractions method, laser-induced fluorescence, and atomic absorption spectroscopy.

Both chapters include commentaries of published papers. I commented on the most important results obtained and the facts that are not usually widely discussed in published articles, like the motivation and issues. Note that the papers are not attached to this work because they are not published in an open-access regime.

1 Spokes in High Power Impulse Magnetron Sputtering

1.1 Introduction

High power impulse magnetron sputtering (HiPIMS) is a physical vapor deposition technique utilizing a short high energy pulse (several 10s of μs) followed by a long off-time to deliver the power into the discharge [1, 2]. It leads to dense plasma formation with a high fraction of ionized species and consequently high ion flux towards the substrate. In HiPIMS discharge, it was observed that in some cases, the plasma is not homogeneously distributed above the target, but it is concentrated in regions of enhanced ionization, called spokes [3, 4, 5], see Figure 1.1. The spokes were observed only for a certain combinations of experimental parameters such as discharge current, operating pressure, target material, and working gas. The high-speed camera made it possible to determine the spoke velocity of around 10 km.s^{-1} , the number of spokes, the transition between spoke modes, and the different characteristic spoke shapes [6]. The same spoke velocity and spoke rotation frequencies of several hundred kHz were obtained using electrical probes and optical monitoring [5, 7].

The first chapter of this habilitation thesis focuses on studying the spoke phenomena in High Power Impulse Magnetron Sputtering. In the first paper AP1, we described the investigation of the oscillations on the cathode voltage and the discharge current, which emerged suddenly and simultaneously during a HiPIMS pulse. Simultaneous measurement of both oscillations and spokes was conducted to find mutual correlations. Paper AP2 determined the spoke shape, number, and velocity for a broad range of experimental conditions in three magnetic field configurations employing a high-speed camera. Additionally, the spokes were investigated by optical emission spectroscopy. Paper AP3 was focused on simultaneous measurements by a high-speed camera and strip probes embedded in the target. Such a dual diagnostics system provides for gaining information on spokes temporal and spatial behavior in HiPIMS plasmas. A correlation between the optical emission image of an individual spoke and the current deliv-

ered to the target by the spoke has been made for a range of magnetron operating conditions. Additionally, merging and splitting of spokes as they rotate has been studied. Paper AP4 investigates quasi-stable spoke configurations evolution during the HiPIMS pulse by simultaneously using six embedded strip probes evenly distributed in the target and by simultaneous observation by a fast camera. This experimental arrangement tracks the changes in the spoke configuration.

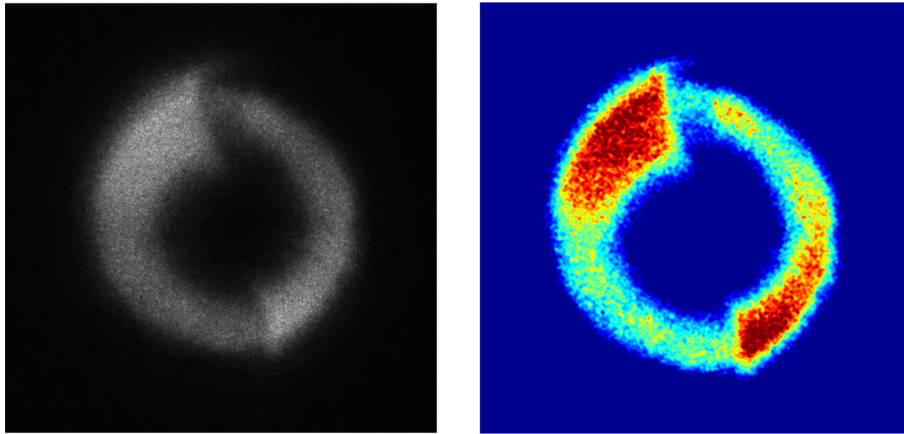


Figure 1.1: Image of the spoke: (left) original grey-scale image from high-speed camera, (right) image converted to (false) color.

1.2 The link between the oscillations of voltage and current induced by spokes

Several HiPIMS discharge investigations showed oscillations on both the cathode voltage and the discharge current at the later stages of the HiPIMS pulse, where the highest discharge current occurs. Figure 1.2 demonstrates an example of such oscillations on cathode voltage and discharge current waveforms. In the literature, the oscillations were detected at various pressures at later stages of the HiPIMS pulse: i) on the cathode voltage for Ta target [8], ii) discharge current for Ti target [9], iii) on cathode voltage and discharge current on Nb [10], LaB₆ [11] and Ti [12] targets. Those oscillations manifest only if a certain target current threshold is reached. This is in line with direct

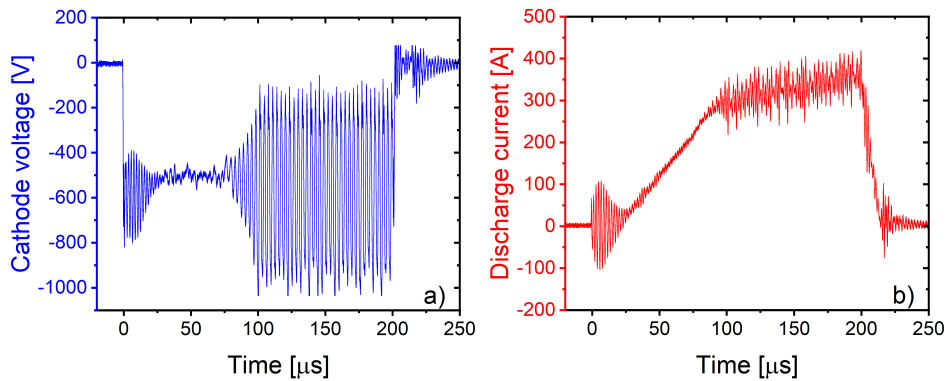


Figure 1.2: Example of oscillations on (a) cathode voltage and (b) discharge current waveforms for the pressure of 1 Pa and titanium target.

observations in the literature, where spokes are only seen above a certain current level for Ti targets [7] and Cr, Cu, Nb, Mo Ta targets [13].

Our investigation aimed to verify whether oscillations are connected to the generator electronics or the spokes. Coincidentally, most examples of oscillations mentioned above were detected, when a commercial HiPIMS power supply made by Melec GmbH company was utilized in the experiments. Because the HiPIMS generator (model SIPP 2000) made by Melec GmbH company was available in our lab, we wanted to carry out the experiments with two differently electronically designed power generators. Therefore, experiments were made in collaboration with dr. Hubička and dr. Čada from the Institute of Physics of the Czech Academy of Sciences in Prague, who supplied a custom-made power generator.

Simultaneous measurement of the cathode voltage and the discharge current oscillations and spoke formation were conducted to find mutual correlations and presented in paper AP1. The relation between the cathode voltage, the discharge current oscillation frequency, and the spoke frequency was investigated. A sputtering system equipped with a 20 cm circular titanium target was used. Two different HiPIMS generators (Melec GmbH and custom made) were employed to drive the HiPIMS discharge. The Melec generator utilized a coil in the arc protection circuit, while the custom made generator used a

resistor. A high-speed intensified charge-coupled device (ICCD) camera PIMAX 3 was applied for discharge imaging. The camera worked in dual-image feature mode, enabling the capture of two snapshots during one HiPIMS pulse with only a $3 \mu\text{s}$ between them. In these and further experiments, we could determine the spokes shape, number, and rotation velocity using the PIMAX 3 camera working in this mode.

We wanted to find the conditions where we observe the cathode voltage and the discharge current oscillations. First, we wanted to find out if the oscillations are caused only by the electronics of the power generator. Therefore, we did not connect power generators to the deposition chamber but specially designed electrical measurement circuits, and we monitored the V-I characteristics. We did not detect oscillations in any set conditions covering all the conditions we used in the real sputtering process. Next, the power generators with the electronics measurement circuits were connected to the deposition chamber, and the HiPIMS discharge was ignited. The oscillations were detected only when an inductance provided by a coil ($> 3.2 \mu\text{H}$) was a part of the electrical circuit, and the discharge was sustained. We concluded that the electronics do not cause the oscillations, but the oscillations are excited in the plasma and amplified by the electrical circuit in the power supplies. We found experimental conditions (working pressure and discharge current) where the oscillations appeared and determined their frequency.

Additionally, we made a model of the real HiPIMS arrangement, including the generator circuit and the discharge. The oscillation source was added to the equivalent electrical circuit representing the discharge. It was found that the model results agreed well with the measured data. Thus, the model confirmed that the source of oscillations is in the HiPIMS plasma.

The fast camera was utilized to capture the spokes for wide range of experimental conditions. From the images we estimated number of spokes and rotation velocity of the spoke. We also derived the spoke rotation frequency from the spoke rotation velocity and racetrack diameter. In our case, the oscillation frequency was one order of magnitude higher than the rotation frequency of the spokes. Moreover, the oscillation frequency and the rotation frequency of spokes showed different evolution with pressure and the discharge current. Thus, a direct connection between the rotational motion of spokes and the

oscillations on the cathode voltage and the discharge current was not found. Nevertheless, we observed that oscillations always accompanied the spokes because we never detected the oscillations without spokes.

1.3 Study of spoke properties in broad range of experimental conditions

The results in the literature on the spoke shape [13, 14, 15, 16, 17], number [3, 5, 7], and rotation velocity [5] suggest that the spoke behavior depends on the experimental configuration. Therefore, comparing the results obtained from two different laboratory devices is difficult, even if the conditions, such as pressure and discharge current density, are similar. We realized this issue while writing the previous article AP1. Therefore, paper AP2 aimed to look at the effect of experimental conditions such as working pressure and discharge current density on spoke appearance and behavior, emphasizing the role of the magnetic field strength.

We used a 7.6 cm circular titanium target and intended to cover broad range of experimental conditions. The working pressure was investigated in the range of 0.1 – 5.0 Pa. It covers the whole range of pressures used for sputter depositions. The applied discharge current density was up to 10 A/cm², which was the limit of the power supply. In this work, three different magnetic field strengths were applied. Such investigation was inspired by previous works [18, 19], where the weakening of the magnetic field strength led to a significant increase in the deposition rate, which was explained by the decrease of the backward flux of ions to the target [19]. The change of the target thickness modified the magnetic field strength at the surface, see Figure 1.3. The PIMAX3 high-speed camera with dual image feature enabled us to determine the spokes shape, number, and velocity.

Until now, most reports described only the triangular and diffusive spoke [16]. We captured thousands of plasma emission images with a fast camera. All images were processed manually, and several spoke shapes were recognized. Therefore, developing a methodology to distinguish different spoke shapes was necessary. The criteria

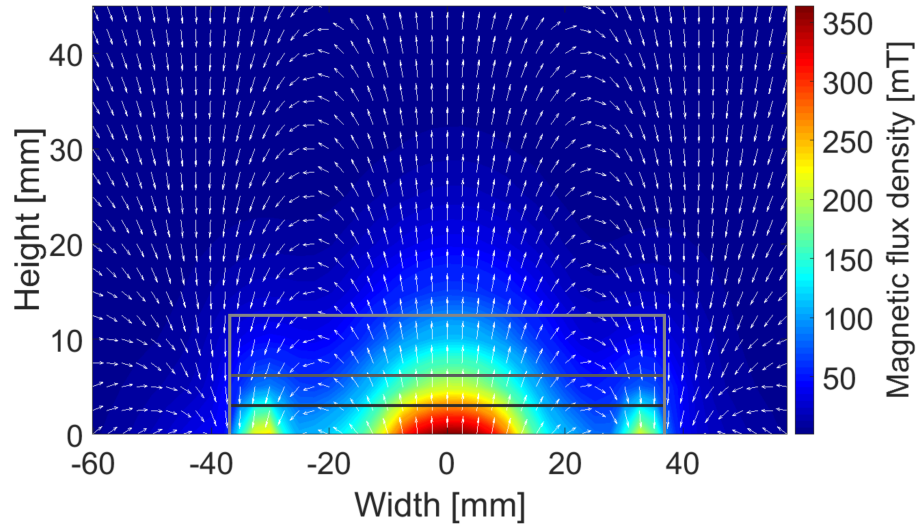


Figure 1.3: Magnetic field configuration map with depicted positions of the targets with different thicknesses.

for determining spoke appearance were developed semi-empirically using dual images focusing on spoke shapes and spoke motion:

1. Non-recognizable spoke – plasma emission is homogeneously distributed without plasma self-organisation.
2. Stochastic spokes – the plasma is self-organized into the rotating spokes without noticeable periodicity, and well-defined spoke borders.
3. Triangular spoke – a narrow trace progressively expanding in width and intensity until a sharp drop of emission signal terminates it. Spokes are uniformly distributed over the racetrack.
4. Diffusive spoke – spokes are elongated and dispersed, with a narrow trace start, the broad middle part of the spoke, and a narrow trailing edge observed. Spokes are uniformly distributed over the racetrack.
5. Round spoke – spoke exhibits round shape with neither the sharp end in plasma emission as triangular spoke nor elongated

dispersed appearance as diffusive spokes. The spokes are uniformly distributed over the racetrack.

The typical image of different spoke shapes is shown in Figure 1.4. For each magnetic field, a map was created relating the spoke shape occurrence with the discharge conditions. In literature, we can find contradicting results, i.e., an increasing number of spokes [3] as well as the decreasing number of spokes [7] with increasing discharge current. Thus, we decided to investigate this issue and find out what was correct. The answer is that both previously reported results are right. We revealed that both the increase and the decrease of the number of spokes with increasing the discharge current could be reached by variation of experimental parameters. Additionally, we reported that the spoke rotation velocity decreased by increasing the pressure and the magnetic field strength. Thus, the number of spokes and spokes velocity were found to strongly depend on the discharge conditions.

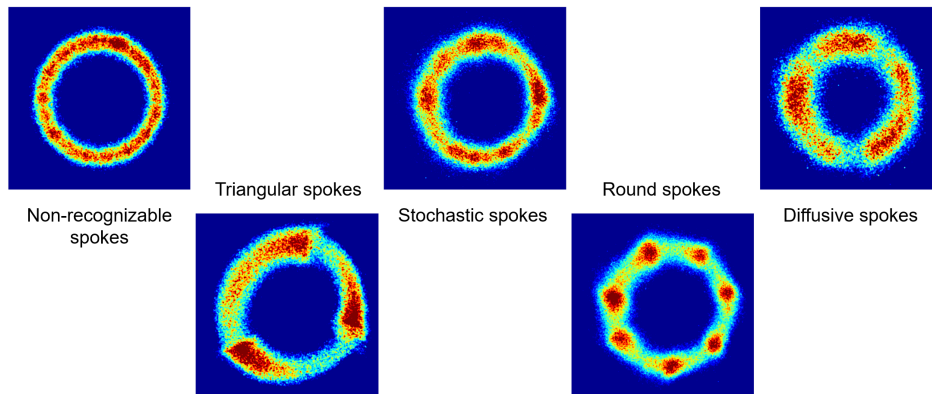


Figure 1.4: Images of characteristic plasma emission.

Our experimental results contradicted the early reported hypothesis [16] that titanium as the target material with the lower second ionization potential should exhibit only a diffusive spoke shape. Both triangular and diffusive spoke shapes were observed for the titanium target in our case. The optical emission spectroscopy revealed that triangular spokes correlated with the strong argon ion emission. The round spokes presence was connected to the decreasing emission of

a titanium ion with increasing discharge current due to the creation of multiply charged ions. We proposed a model which describes the spoke shapes based on these findings. In our model, a triangular spoke shape is formed due to secondary electron production induced by argon ions from the spoke sides. The magnetic field then traps these electrons, forming a distinct trailing edge. Round spokes are created by the secondary electrons generated within the spoke by the impact of multiple ionized metal ions. Mapping the spoke properties led to their systematic description, which had been missing until then. Additionally, we used newly gained information about spokes to improve the spoke model used so far.

1.4 Spoke splitting and merging observed by high-speed camera and strip probes

Group of prof. Bradley from Liverpool University detected periodic oscillations in the local target current density by electrical isolated (strip) probes embedded in the target and attributed these oscillations to the presence of rotating spokes [20]. However, visual confirmation of spokes presence was not possible in their arrangement. Since the high-speed camera proved to be a powerful instrument for spoke investigation, we carried out joint experiments, where we wanted to confirm that observed strip probe current modulations are indeed due to spokes. Therefore, simultaneous electrical and optical measurements in HiPIMS plasma were performed in a joint investigation with prof. Bradley and his Ph.D. student in our lab.

In this study AP3, we employed a 7.6 cm circular niobium target. The strip probes embedded in the target enabled us to observe a distinct modulation in the local target current density as the spokes pass over a particular target region. Three strip probes, made of the target material, were placed in machined slots at three angular positions of 25° from each other around the target, see Figure 1.5. They are always at the same potential as the target, which makes them indistinguishable for the plasma from the rest of the target. The strip probes extended beyond the target edge to allow electrical connections to the power supply. A thin layer of polyimide tape was wrapped around three sides of the stripe probes to isolate them electrically from the

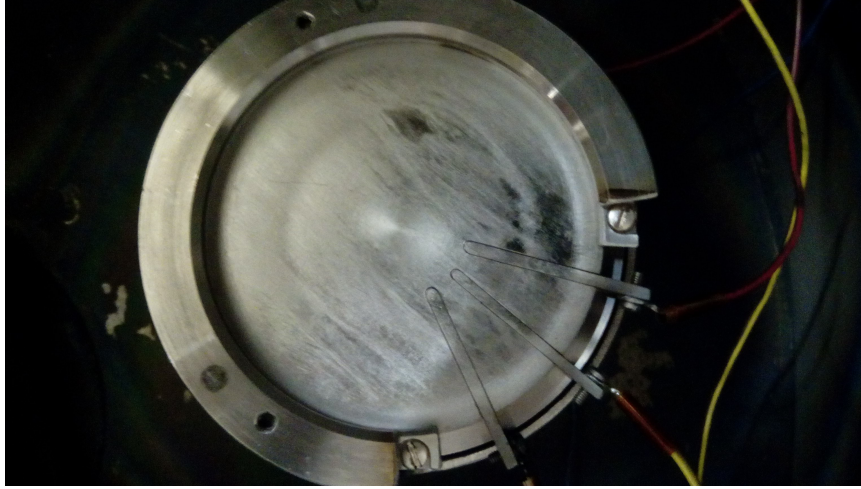


Figure 1.5: Experimental arrangement of the strip probes from the top view.

rest of the target. This is tricky because the tape is very thin, and the space between the probe and the target is tight. Additionally, the tape should not rise up, and the strip probes should be at the same level as the target to prevent arcing on the sharp edges. Note that discharge current reached up to 240 A, i.e., 5.3 A/cm^2 . Thus, correctly placing the embedded probes was critical to the entire experiment. Simultaneously, we detected the plasma emission from the top by high-speed camera PIMAX3 .

We revealed that high-speed camera imaging and embedded strip probes in the target show identical profiles of passing spoke structures with a sharp trailing edge, see Figure 1.6. Such a diagnostic system allows us to get information about the discharge above the whole target surface by camera imaging twice per HiPIMS pulse and simultaneously get data from three localized places above the target using embedded strip probes during the same HiPIMS pulse. We utilized this experimental setup consisting of the camera and strip probes to investigate time-resolved spoke dynamics. We revealed that the number of spoke changes during the single pulse. For the first time, we captured both the merging and splitting of a set of spokes as they rotate. After merging or splitting events, the new spoke configuration was not always stable in time. During these measurements, a large

spoke could be divided into two smaller spokes only to merge a short time later. These observations confirmed that the spokes are a dynamic phenomenon.

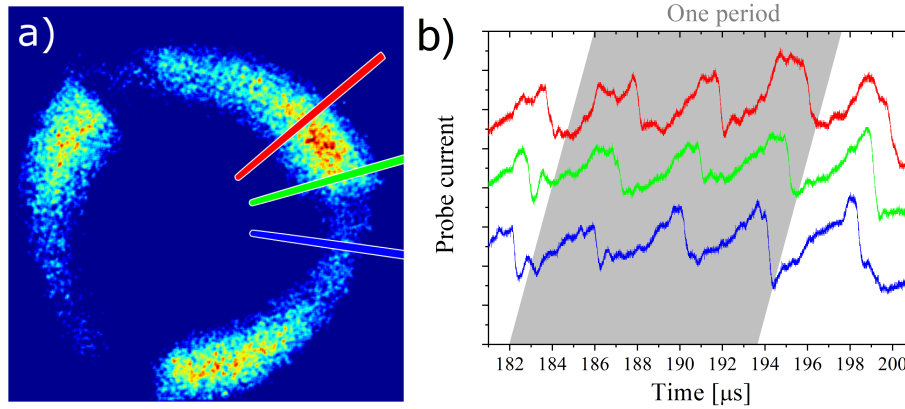


Figure 1.6: 2D plasma emission image (a) of the whole target taken by high-speed camera at $191 \mu\text{s}$ with positions of the strip probes (red, green and blue) and (b) the corresponding strip probe waveforms for working pressure of 0.14 Pa . One spoke rotation period is illustrated by the grey background.

Furthermore, we developed a simple phenomenological model, which relates the stable configuration of spokes to their dimensions, rotation velocity, and the background Ar gas atoms velocity. The model estimates the number of spokes that can be sustained for particular plasma conditions. The model still holds because no contradicting report occurs in the literature. An in-depth study of the spoke configuration was performed later and discussed in the text hereafter.

1.5 In-depth investigation of spoke configuration

The results in paper AP3 revealed that as the spokes rotate above the target, their properties can change over time, with frequently occurring splitting or merging. Applying our knowledge about spoke shape and configuration gained from earlier experiments AP2, we further extend all these investigations as we intended to study the changes in spoke configuration more deeply AP4.

1. SPOKES IN HIGH POWER IMPULSE MAGNETRON SPUTTERING

In this study AP4, the cooperation with prof. Bradley continued. We planned to utilize a niobium target with six embedded strip probes evenly distributed over the target, as shown in Figure 1.7(a), together with the high-speed camera. Such probe arrangement leads to tracking the changes in the spoke configuration around the racetrack at any moment in time. However, the standard anode prevents the installation of the strip probes. We made a few measurements without any anode, but we were not satisfied with the stability and repeatability of the experiments. Therefore, we designed a custom-made anode elevated a few millimeters above the target surface, which could be utilized with the strip probes, see Figure 1.7(b). Based on our previous paper AP2, we chose to study (a) the low-pressure case (0.2 Pa), where the triangular spoke should be present, and the high-pressure case (4 Pa), where the round spoke should occur. A $2.4\ \Omega$ resistor integrated into series with a cathode worked as negative feedback limiting the runaway of the discharge current. Thus it increased the stability of the discharge current.

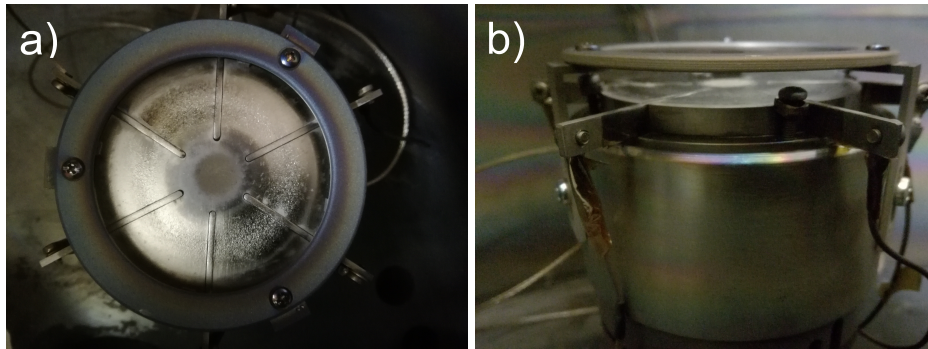


Figure 1.7: Experimental arrangement from the top view (a) and the side view (b) on the slotted target outfitted with six strip probes.

Since we had signals from 6 localized places above the target, it was necessary to get information about the spoke configuration from the rest of the target. At first, all six strip probe current signals were processed to recreate the spoke configuration at any point of time during the HiPIMS pulse. After that, the spoke configuration rotational velocity was determined during the pulse at the positions of the probes using a processing script. Afterward, the rotation velocity temporal

evolution was used to transform the data to a frame rotating with the spokes. Virtual data points between the probes were found from interpolation. An example of a reconstructed spoke configuration is illustrated in Figure 1.8, where the color scale from blue to red is adjusted for the current minima and maxima, respectively. The figure shows us from 65 to 135 μs seven spokes. At 135 μs , we can detect the merging of two spokes and simultaneously the splitting of one spoke.

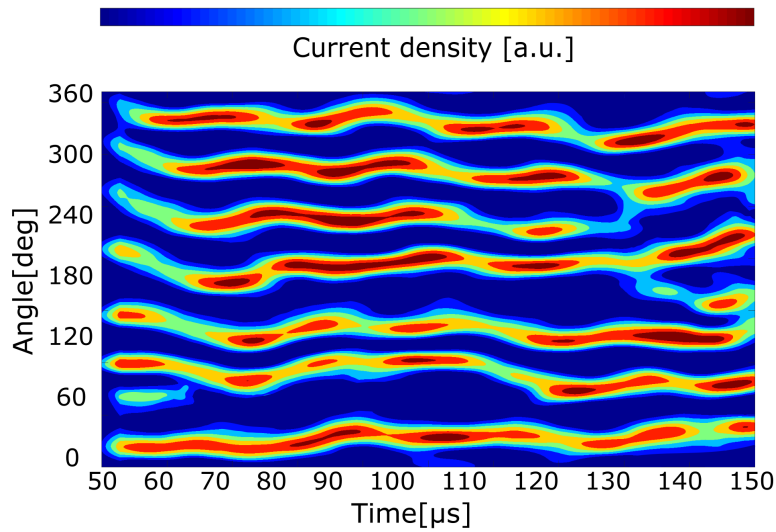


Figure 1.8: An example of the reconstructed spoke configuration during the pulse from 50 to 150 μs at the pressure of 4 Pa.

We recorded around 150 pulses under the same experimental conditions to obtain sufficient statistical data. We identified several possible scenarios of spoke behavior during the HiPIMS pulse using images with reconstructed spoke configuration. The merging and splitting events occurred in various combinations on different target parts, either successively or seemingly simultaneously. The merging and splitting of spokes was discovered to influence the neighboring spokes. For the low-pressure case (0.2 Pa), the most probable configuration was four spokes, with an equal probability for spokes to merge and split. In the high-pressure case (4 Pa), the spoke configuration exhibited a higher number of spokes, i.e., 7 or 8 spokes. An increasing number of spokes with increasing pressure corroborates well with our

previously reported results using titanium target AP2. Furthermore, we observed a significantly higher occurrence of spoke splitting versus spoke merging during a single pulse.

We also created a model that includes the stable spoke configuration, spoke splitting, and spoke merging. Anders phenomenological model [14] served as an inspiration for us. We assumed: i) electrons rotating in $E \times B$ ionised sputtered metal, ii) metal ions are back-attracted to the target, and iii) re-sputtering. We described the spatial evolution of electrons, Nb atoms, and Nb ion concentration in the stable spoke in the model. Then we showed how the small perturbation in Nb atom concentration could evolve in time, and a new spoke is formed. Thus, we described how the spoke can split. Similarly, the model can explain the spoke merging in the reverse case.

1.6 Conclusion

This section was devoted to the investigation of the spoke phenomenon using optical emission spectroscopy, high-speed camera, and strip probes. An extensive study of spoke images for various pressures, discharge currents, and magnetic fields led to the development of a methodology that allowed us to categorize spoke based on its appearance. The results from strip probes showed us how dynamic phenomenon spokes are and that a statistical approach is needed to study them. In the future measurements, the experimental data describing the plasma parameters inside the spokes are required to better understand the spoke phenomenon. At the same time, due to the high power load, all diagnostics must be non-invasive, making the spoke investigation still a big challenge.

2 Dynamics of sputtered particles in High Power Impulse Magnetron Sputtering

2.1 Introduction

A deep understanding of the physical processes driving the HiPIMS discharge is essential for optimizing thin-film growth and developing even more efficient sputtering processes with an enhanced level of discharge control. Only a few techniques suitable to follow the temporal and spatial evolution of sputtered species densities have been developed, such as atomic absorption spectroscopy or laser-induced fluorescence [21, 22].

We want to use a simpler method to determine the density of sputtered species as well as the method that does not disturb the plasma. However, the sputtered species in the ground or metastable states do not emit any direct optical signal, and it is difficult to obtain information about the number densities of the species in these levels from optical emission spectroscopy. Thus, we developed an indirect method based on self-absorption [23, 24] to determine the number densities of sputtered species in the discharge.

This chapter concentrates on the study of HiPIMS processes utilizing the effective branching fraction (EBF) method, laser-induced fluorescence (LIF) imaging, and atomic absorption spectroscopy (AAS). The methods mentioned above have been used to determine the ground state number density of Ti atoms and ions. In paper AP5, we applied the effective branching fractions method to determine the ground state densities of the sputtered titanium atoms and ions and the evolution of titanium atoms and ion densities in three cases ranging from the direct current (dc) driven sputter process to HiPIMS. The following paper AP6 deals with the density evolution of sputtered species determined by EBF in single and multi-pulse HiPIMS. Moreover, the results obtained by the EBF method were compared to results determined using the tunable diode-laser absorption spectroscopy (TD-LAS) in the dc case. Papers AP7 and AP8 were published simultaneously. These extended and detailed experimental studies of HiPIMS processes were performed by time-resolved imaging of the ground state sputtered

particles. Paper AP7 focuses on the role of main discharge parameters, such as pulse repetition rate and pulse energy. Paper AP8 deals with the effects of the plasma-on phase for different plasma pulse duration, pulse energy, gas pressure, and molecular oxygen admixture.

2.2 Optical diagnostics for characterization of sputtering process

There are plenty of non-radiating species in the ground states in sputtering discharges. It is challenging to acquire the number densities of the species in these states from optical emission spectroscopy. But how do we measure them non-destructively and easily? A method based on self-absorption has been invented to estimate the number densities of argon [25, 26] and neon [26, 27] metastable states in low-temperature plasma. We adopted this method using effective branching fractions and determined the density of non-radiating species from the intensities of self-absorbed spectral lines.

In paper AP5, we introduced the effective branching fractions (EBF) method to determine the sputtered titanium atoms and ions ground state densities. The procedure is based on fitting the theoretically calculated branching fractions to experimentally measured ratios of the relative intensities of selected lines of the measured species. At first, it was necessary to choose the suitable candidates for the titanium atom and ion lines from the NIST database [28], fulfilling the condition of one transition going to the ground state. Then we have to find these lines in an overview spectrum. The lines should be easily measured and not overlap with surrounding spectral features in the measured spectra. Additionally, they have to exhibit a high transition probability (Einstein coefficient). An example of the branching fraction fit used to determine Ti atom density is presented in Figure 2.1. In this case, the best fit of theoretically calculated branching fractions to the experimentally measured ratios of the relative intensities is achieved when the Ti atom density is $1 \times 10^{17} \text{ m}^{-3}$. Such a result is comparable with the density reported in the literature [29].

The manuscript AP5 also presented the lists of carefully selected Ti atom and Ti ion lines applied for density determination. However, it is not necessary to use all the lines summarized in Table I and Table II

in the paper AP5. For example, we took 13 lines of Ti atoms and 19 lines of Ti ions and utilized them for the several case studies, where we applied EBF method to estimate:

1. The titanium atom density dependence on the power and working pressure in a dc magnetron sputtering discharge.
2. Titanium atom and ion densities for the transition from dc to HiPIMS regime.
3. Temporal evolution of titanium atom and ion densities during short and long HiPIMS pulse.

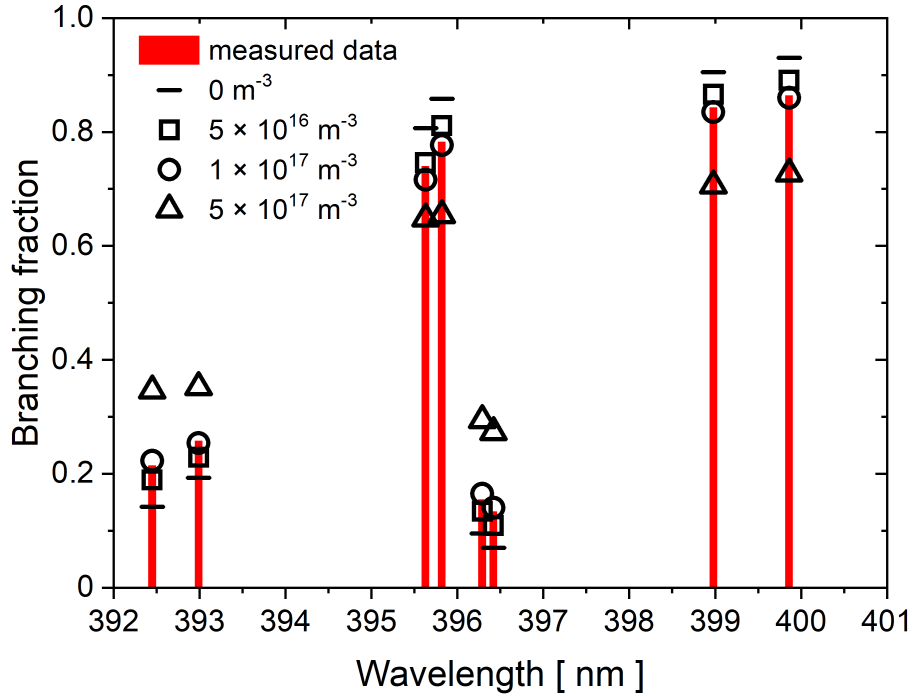


Figure 2.1: The effective branching fraction fit used to determine Ti atom density. Calculation was done for $z = 5$ cm, $T_{\text{exc}} = 3000$ K, $T_{\text{gas}} = 300$ K.

For the measurements of the first two cases, we utilized a charge-coupled device (CCD) detector, while for the temporal evolution of

sputtered species in the HiPIMS pulse, we applied an ICCD detector. The relative uncertainty of density determination was about 5% for measurements made by the CCD detector. In contrast, for time-resolved measurements made by the ICCD detector, it was around 15% in our experimental setup. Note that these uncertainties are determined statistically by the fitting procedure from the residual sums of squares.

We measured the titanium atom and ion lines and determined the densities for all three case studies. It was difficult to compare the densities in some cases since different experimental setups, magnetic fields, and in the case of HiPIMS, different peak discharge currents or pulse lengths were used. Nevertheless, determined Ti atom and ion densities and the evolution of Ti atom density with the applied power and pressure were comparable to those in the literature, proving that the EBF method gives reliable data in sputtering discharges. The EBF method does not require any reference source, i.e., a lamp or a diode laser. The Ti atom and ion densities are determined directly from optical emission spectroscopy signals. The OES measurement is simple and enables us to implement the EBF method into any sputtering experiments. Only a vacuum feed-through or a window for optical fiber, together with a spectrometer with sufficient resolution, is required for the measurement. Thus, the EBF method enables investigation of the time-resolved dynamics of sputtered species simply, reliably, and without plasma disturbing.

2.3 Diagnostics of standard and multi-pulse HiPIMS discharge

The main disadvantage of HiPIMS is a low deposition rate compared to the direct current magnetron sputtering (dc-MS) for an equivalent average applied power [30] and, consequently, a longer process for the same thickness when this technique is used on an industrial scale. Therefore, a deposition rate increase would make the deposition process more economical and efficient, while the deposited thin film properties would be maintained or even enhanced compared to dc-MS. Recently, several single-pulse HiPIMS (s-HiPIMS) were put close to each other, creating a package of pulses [31]. Thus the HiPIMS was op-

erated in the so-called chopped [31], burst [11], or multi-pulse regime (m-HiPIMS) [32]. It was demonstrated that the deposition rate in m-HiPIMS could be significantly higher for the same average power than in s-HiPIMS [33]. The tailoring of the multi-pulse sequences allows for further tuning of the deposition process. Using the m-HiPIMS, the first results showing changes in coating structure and characteristics have already been published [33, 34].

The initial results were reported mainly on the thin film deposition by m-HiPIMS with limited plasma diagnostics and an understanding of the sputtering process. Therefore, we decided to investigate the multi-pulse HiPIMS by the EBF technique in this paper AP6. Ti atom and ion densities determined in m-HiPIMS were compared to the densities in a single-pulse HiPIMS. Moreover, we compared the results acquired by the EBF method with those obtained from the well-established TD-LAS method. TD-LAS is a sophisticated and expensive method that requires an experienced researcher. Therefore, we conducted the experiments in the lab of prof. Minea at the University Paris-Saclay in France, in cooperation with dr. Vitelaru from the National Institute for Optoelectronics in Romania.

A cylindrical vacuum chamber equipped with a 10 cm circular titanium target was used in these experiments. Simultaneous measurements of TD-LAS and EBF methods were conducted in the same investigated volume. The number densities of Ti atom were measured as a function of the discharge current and the working pressure. It was demonstrated that Ti atom number densities determined by the EBF method and TD-LAS agree throughout the investigated conditions. The agreement between the EBF method and TD-LAS technique results can be taken as the validation of the EBF method by another independent measurement. The EBF method proved to be a reliable technique for the Ti atom number density determination. A similar comparison was not performed for Ti ions due to the low signal of Ti ion lines. However, because the EBF method is independent of the charge and the calculation procedure principle is the same for Ti atoms and Ti ions, the method can also be used in Ti ion number density measurements.

The multi-pulse HiPIMS investigation was performed using the titanium target with a diameter of 20 cm. The study was focused on the simplest case, where the pulse sequence was composed of two pulses.

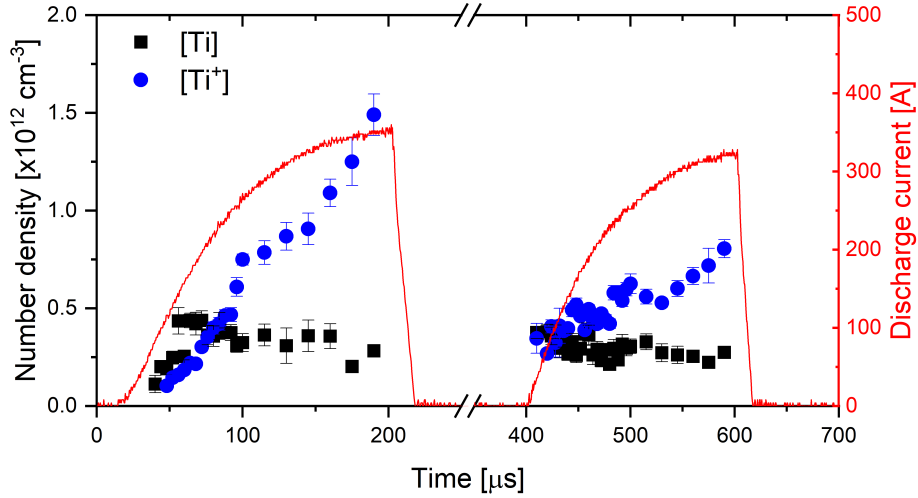


Figure 2.2: The discharge current, the number density of Ti atoms and Ti ions in m-HiPIMS discharge. The delay between the first and the second pulse was set to 200 μs . The operation pressure was set to 5 Pa, the pulse duration of both pulses to 200 μs and the period to 100 ms.

The pulse duration was set to 200 μs with discharge current peaking around 350 A (1.1 A/cm^2), because we could easily detect titanium atoms and ions for such parameters as reported in our previous paper AP5. The delay time between pulses in the pulse sequence was set to 200, 400, and 1500 μs . We expected that the first pulse would influence the second pulse in the pulse sequence because remaining charged carriers will make discharge ignition in the second pulse easier. Additionally, the sputtered species from the first could also be available for ionization during the second pulse. The total number of pulses per second was kept constant as we planned to compare the results obtained from s-HiPIMS and m-HiPIMS.

The Ti atom and ion density evolution showed that the residual titanium atoms and ions from the first pulse are crucial for the initiation and development of the second pulse, see Figure 2.2. The residual titanium atoms produced by the first pulse are already thermalized at the beginning of the second pulse and can be ionized during the second pulse. The discharge current rises faster in the second pulse but does not reach the same maximum as the first pulse, see Figure 2.2. The time evolution of the titanium atom density showed different behavior.

The initial increase is followed by a decrease in the first pulse, while a relatively constant progression during the second pulse is observed. The Ti ion number density steadily increased during both the first and second pulse, while the increase was steeper in the first pulse.

For the delay of 400 μs , the evolution of Ti atom and ion was similar as for the 200 μs delay. Only the reservoir of thermalized atoms gets depleted as the delay increases. Surprisingly, we still detected the sputtered Ti atom for the delay of 1500 μs , and the evolution of the Ti atom during the second pulse was similar to shorter delays. For this longest investigated delay, Ti ion evolution was the same as in the case of the first pulse.

From the deposition point of view, we found out that the ionization fraction of sputtered species is still very high in the m-HiPIMS case reaching always more than 75%. The total ion flux to the substrate increased by more than 40% in m-HiPIMS with 200 μs delay compared to s-HiPIMS. However, we must keep in mind that we measured the overall ion flux of Ti ions and Ar ions. We can speculate that the delay of 200 μs is not long enough for Ar gas to replenish, and this increase could be attributed mostly to the Ti ions. This could be quickly resolved by additional measurements using the biasable quartz crystal monitor, which can measure total ion and atom flux or total atom flux of titanium and thus determine the role of titanium ions. Additionally, at least 20% increase in deposition rate was detected in m-HiPIMS compared to s-HiPIMS, which is in agreement with results reported in literature [33].

The above mentioned results showed that the delay between pulses in the pulse sequence plays a crucial role in ion flux to substrate enhancement. Additionally, using the m-HiPIMS instead of a single-pulse HiPIMS led to an increase in the deposition rate and thus increased HiPIMS technology efficiency. Since we studied the simplest multi-pulse HiPIMS case, there is a potential for further improvements. On the other hand, more parameters make the whole sputtering process more complicated and open more questions, such as what pulse duration, the delay between the pulses, or the number of pulses should be the best or optimal for a particular deposition process.

2.4 Spatial and temporal density evolution determined by LIF and AAS measurements

During our previous works AP5, AP6, we realized that comparing experimental results such as sputtered particle densities in the literature is difficult and sometimes not even possible. The reason is that different laboratories use different experimental setups, magnetic field configurations, pulse lengths, repetition rates, working pressures, etc. Until 2020, an overview article, which covers the time and spatially-resolved density evolution of sputtered species in a broad range of experimental conditions, did not exist. Therefore, we intended to systematically investigate the time-resolved ground state sputtered particles in HiPIMS discharge in a different position from the target surface. For this complex research, we established a collaboration with dr. Britun and prof. Snyders from the University of Mons in Belgium. They had experience with two-dimensional time-resolved density mapping of the ground state titanium neutrals and ions by laser-induced fluorescence (LIF) [21, 22]. In our joint investigation AP7, AP8, we focused on the role of main discharge parameters such as pulse duration, repetition rate, plasma pulse energy, gas pressure, and molecular oxygen admixture effects. The behavior of neutral and singly ionized atoms were studied during the plasma-on and plasma-off time phases.

The experiments were carried out in the lab of prof. Snyders at the University of Mons in Belgium. Two balanced magnetron sources equipped with circular planar titanium targets, one of 7.6 cm in diameter and the other of 10 cm in diameter, have been used. For diagnostics, we utilized LIF imaging for two-dimensional time-resolved density mapping of the ground state titanium neutrals and ions together with AAS.

It is desirable to gather the information from the proximity of the target surface. However, the standard anode prevents observing the ionization region, an essential part of the discharge, where the sputtered species are ionized. Thus, we adopted our custom-made anode utilized in the experiments with strip probes AP4. Moreover, we made the anode thinner (about 1 mm) to keep the shielded area as small as possible, see Figure 2.3.



Figure 2.3: Magnetron head configuration with custom-made anode.

For part of the investigation in paper AP7, we utilized this newly designed anode geometry, which allowed the laser beam to touch of the cathode surface. It enables particle visualization close to the target surface as shown in Figure 2.4, where the typical example of the ground state density distribution for sputtered Ti neutrals and ions above the magnetron target in the dc and HiPIMS case is presented. The ground state density is calibrated by the AAS method. We chose a logarithmic density representation for Ti neutral and ion density. In this representation, a single color step corresponds to a threefold density change. It enables us to visualize the particle behavior up to 10 ms after the end of the HiPIMS pulse, where densities are three orders of magnitude lower than in plasma-on time. The left column in Figure 2.4 shows a homogeneous distribution of Ti atoms (upper image) and a very low density of the Ti ions. On the right upper image in Figure 2.4, we can observe that ground-state neutral atoms being ejected from the target during the plasma-on time with maximal density at 1 – 2 mm above the target surface. As the sputtered titanium atoms enter the ionization zone, i.e., moving away from the target, they are ionized, and we can observe a significant reduction in the titanium atom density. The depletion zone coincides with higher Ti ions density, as demonstrated in the lower right image. The *ionization zone* is identified in these two papers AP7, AP8 as the area above the target where electrons are confined, creating titanium ions.

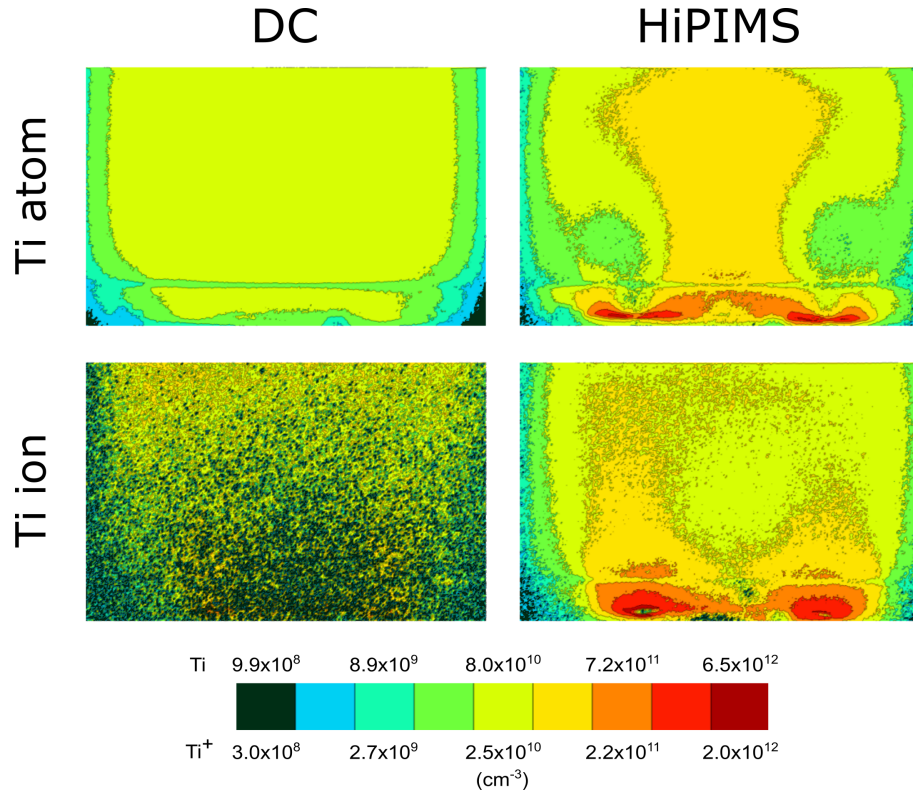


Figure 2.4: Ground state density distributions for Ti neutrals and Ti ions measured above the magnetron target for dc and HiPIMS case. Data were averaged over 30 laser pulses. The pressure was set to 2.7 Pa. The log-color scale is used.

Our motivation for investigating the repetition rate effect comes from our previous paper AP6, where we discovered that the second pulse in the pulse sequence could be influenced by the first pulse even when 1500 μs delay between them is applied. As AAS and LIF measurements enable us to study plasma-on, and plasma-off time, i.e., they were ideal for such research. We observed that increasing the repetition rate from 50 to 400 Hz leads to an increased residual density of the sputtered species, which agrees with our previously reported results AP6. At the same time, the space-averaged ionization fraction remains the same regardless of the plasma repetition rate. The ionization gets uniform in the studied region after about 1500 μs from

the pulse beginning, no matter the pulse repetition rate, which implies a fast particle thermalization.

We also investigated the particle propagation dynamics using the vector diagram approach, representing the density gradients for both sputtered neutrals and ions along with their temporal changes. This approach confirmed the idea of in-flight ionization of the sputtered neutrals. The same order of magnitude values was found for neutrals and ions at the beginning of plasma pulse, nevertheless having an opposite sign.

In paper AP7, we also compared the titanium atom and ion number density gained by the AAS method with the results obtained from the EBF method. An agreement between results obtained by these two techniques (AAS and EBF) has been found. At this point, the EBF method was cross-checked by absorption spectroscopy in two different labs showing that the EBF method is a reliable technique for determining titanium atom and ion number density in magnetron sputtering discharge.

The missing information in this work is the density evolution of argon ions, as they play a crucial role in the sputtering of the target. Based on the literature, we tested different excitation wavelengths by the LIF. Despite the great effort, we did not successfully detect any signal from argon ions. Therefore, future work should focus on this subject.

Furthermore, we examined the influence of plasma pulse duration, pulse energy, gas pressure, and molecular oxygen admixture by LIF technique, focusing on the plasma-on time AP8. This paper was published simultaneously with the paper AP7, and we considered it its extension. In this study AP8, only the anode covering the ionization region, i.e., the area close to the target surface, was used. For each experiment, we created time-resolved 2D number density maps of titanium atoms and titanium ions. In addition to the density maps, the ionization fraction (IF) maps have been built for all studied conditions. The IF has been calculated based on the calibrated LIF data by the AAS technique. We also further processed the LIF images to get additional information. After applying the Abel transformation, the space-averaged density of the titanium atoms and titanium ions were calculated from the imaged region.

Since we investigated a broad range of experimental conditions a short summary of the most important result follows:

- LIF mapping shows the ground state density evolution, both for neutrals and ions.
- The maximum ionization corresponds to the shortest applied pulse for the same applied pulse energy.
- The ion production may increase by a factor of 2.5, while the neutral density may drop 1.5 times when the pulse energy is doubled.
- The area above the target surface corresponding to high IF values shrinks with increasing argon pressure.
- An order of magnitude lower density of neutrals and ions is observed as a result of only a fourfold pressure decrease.
- In the poisoned regime, a decrease in titanium neutral and ion ground state densities was seen throughout the investigated region of interest. Titanium ion density is decreased 30 times with a 10% oxygen admixture.
- The ionization fraction itself is found to be higher in the poisoned regime, while the spatial distributions of the sputtered atoms in both reactive and non-reactive cases are very similar.

These two joint papers AP7, AP8 enable us to compare the particle dynamics in very different experimental conditions, which was the goal of this research. Additionally, we showed that using a custom-made anode allowed us to observe and investigate the area directly above the target (ionization region), where the atoms are sputtered from the target and consecutively ionized. Until now, the models only theoretically investigated this ionization region. Thus, the experimental results presented in paper AP7 could be further utilized to verify and improve the ionization region model [35] dealing with time-dependent volume-averaged plasma chemical description of the ionization region in close vicinity of the target racetrack.

2.5 Conclusion

This section presented a simple, non-invasive optical method for studying the magnetron sputtering process. This method, called the effective branching fraction method, enabled us to determine the density of titanium atoms and titanium ions. We applied this method to direct current magnetron sputtering, single pulse and multi-pulse HiPIMS plasma. The results of this method coincided both quantitatively and qualitatively with the results from the literature and the results from atomic absorption spectroscopy. Afterward, we studied the spatial and temporal density of sputtered species from the target to the substrate using the EBF method as well as LIF and AAS techniques. These investigations brought essential information that contributed to the understanding of the HiPIMS discharge. Moreover, the results from multi-pulse HiPIMS showed that such an approach could be suitable for sufficient ionization of the sputtered particles at an adequately high deposition rate.

Bibliography

1. HELMERSSON, Ulf; LATTEMANN, Martina; BOHLMARK, Johan; EHIASARIAN, Arutiun P; GUDMUNDSSON, Jon Tomas. Ionized physical vapor deposition (IPVD): A review of technology and applications. *Thin Solid Films*. 2006, vol. 513, no. 1, pp. 1–24.
2. GUDMUNDSSON, Jon Tomas. The high power impulse magnetron sputtering discharge as an ionized physical vapor deposition tool. *Vacuum*. 2010, vol. 84, no. 12, pp. 1360–1364.
3. KOZYREV, Andrey Vladimirovich; SOCHUGOV, N. S.; OSKOMOV, Konstantin Vladimirovich; ZAKHAROV, Aleksandr Nikolaevich; ODIVANOVA, A. N. Optical Studies of Plasma Inhomogeneities in a High-Current Pulsed Magnetron Discharge. *Plasma Physics Reports*. 2011, vol. 37, pp. 667–673.
4. ANDERS, André; NI, Pavel; RAUCH, Albert. Drifting localization of ionization runaway: Unraveling the nature of anomalous transport in high power impulse magnetron sputtering. *Journal of Applied Physics*. 2012, vol. 111, no. 5, p. 053304.
5. EHIASARIAN, Arutiun P.; HECIMOVIC, Ante; DE LOS ARCOS, Teresa; NEW, R.; SCHULZ-VON DER GATHEN, Volker; BÖKE, Marc; WINTER, Jörg. High power impulse magnetron sputtering discharges: Instabilities and plasma self-organization. *Applied Physics Letters*. 2012, vol. 100, no. 114101, p. 114101.
6. HECIMOVIC, Ante; VON KEUDELL, Achim. Spokes in high power impulse magnetron sputtering plasmas. *Journal of Physics D: Applied Physics*. 2018, vol. 51, no. 45, p. 453001.
7. WINTER, Jörg; HECIMOVIC, Ante; DE LOS ARCOS, Teresa; BÖKE, Marc; SCHULZ-VON DER GATHEN, Volker. Instabilities in high-power impulse magnetron plasmas: from stochasticity to periodicity. *Journal of Physics D: Applied Physics*. 2013, vol. 46, no. 8, p. 084007.

8. BOHLMARK, Johan; HELMERSSON, Ulf; VANZEELAND, Michael; AXNÄS, Ingvar; ALAMI, Jones; BRENNING, Nils. Measurement of the magnetic field change in a pulsed high current magnetron discharge. *Plasma Sources Science and Technology*. 2004, vol. 13, no. 4, p. 654.
9. ANDERSSON, Joakim; EHIASARIAN, Arutun P; ANDERS, André. Observation of Ti 4+ ions in a high power impulse magnetron sputtering plasma. *Applied Physics Letters*. 2008, vol. 93, no. 7, p. 071504.
10. ANDERS, André. Discharge physics of high power impulse magnetron sputtering. *Surface and Coatings Technology*. 2011, vol. 205, S1–S9.
11. FRANZ, Robert; CLAVERO, César; BOLAT, Rustem; MENDELSBERG, Rueben; ANDERS, André. Observation of multiple charge states and high ion energies in high-power impulse magnetron sputtering (HiPIMS) and burst HiPIMS using a LaB₆ target. *Plasma Sources Science and Technology*. 2014, vol. 23, no. 3, p. 035001.
12. MASZL, Christian; BREILMANN, Wolfgang; BENEDIKT, Jan; VON KEUDELL, Achim. Origin of the energetic ions at the substrate generated during high power pulsed magnetron sputtering of titanium. *Journal of Physics D: Applied Physics*. 2014, vol. 47, no. 22, p. 224002.
13. DE LOS ARCOS, Teresa; LAYES, V; GONZALVO, Y Aranda; SCHULZ-VON DER GATHEN, Volker; HECIMOVIC, Ante; WINTER, Jörg. Current–voltage characteristics and fast imaging of HPPMS plasmas: transition from self-organized to homogeneous plasma regimes. *Journal of Physics D: Applied Physics*. 2013, vol. 46, no. 33, p. 335201.
14. ANDERS, André. Self-organization and self-limitation in high power impulse magnetron sputtering. *Applied Physics Letters*. 2012, vol. 100, no. 224104, p. 224104.
15. ANDERS, André; PANJAN, Matjaž; FRANZ, Robert; ANDERSSON, Joakim; NI, Pavel. Drifting potential humps in ionization zones: the “propeller blades” of high power impulse magnetron sputtering. *Applied Physics Letters*. 2013, vol. 103, no. 14, p. 144103.

16. HECIMOVIC, Ante; BÖKE, Marc; WINTER, Jörg. The characteristic shape of emission profiles of plasma spokes in HiPIMS: the role of secondary electrons. *Journal of Physics D: Applied Physics*. 2014, vol. 47, no. 10, p. 102003.
17. BREILMANN, Wolfgang; EITRICH, A; MASZL, Cristian; HECIMOVIC, Ante; LAYES, Vincent; BENEDIKT, Jan; VON KEUDELL, Achim. High power impulse sputtering of chromium: correlation between the energy distribution of chromium ions and spoke formation. *Journal of Physics D: Applied Physics*. 2015, vol. 48, no. 29, p. 295202.
18. MISHRA, Anurag; KELLY, Peter; BRADLEY, James W. The evolution of the plasma potential in a HiPIMS discharge and its relationship to deposition rate. *Plasma Sources Science and Technology*. 2010, vol. 19, no. 4, p. 045014.
19. ČAPEK, Jiří; HÁLA, Matej; ZABEIDA, Oleg; KLEMBERG-SAPIEHA, Jolanta-Ewa; MARTINU, Ludvik. Deposition rate enhancement in HiPIMS without compromising the ionized fraction of the deposition flux. *Journal of Physics D: Applied Physics*. 2013, vol. 46, no. 20, p. 205205.
20. POOLCHARUANSIN, Phitsanu; ESTRIN, Francis Lockwood; BRADLEY, James W. The use of segmented cathodes to determine the spoke current density distribution in high power impulse magnetron sputtering plasmas. *Journal of Applied Physics*. 2015, vol. 117, no. 16, p. 163304.
21. BRITUN, Nikolay; PALMUCCI, Maria; KONSTANTINIDIS, Stephanos; SNYDERS, Rony. Particle visualization in high-power impulse magnetron sputtering. I. 2D density mapping. *Journal of Applied Physics*. 2015, vol. 117, no. 16, p. 163302.
22. BRITUN, Nikolay; PALMUCCI, Maria; KONSTANTINIDIS, Stephanos; SNYDERS, Rony. Particle visualization in high-power impulse magnetron sputtering. II. Absolute density dynamics. *Journal of Applied Physics*. 2015, vol. 117, no. 16, p. 163303.
23. HOLSTEIN, To. Imprisonment of resonance radiation in gases. *Physical Review*. 1947, vol. 72, no. 12, p. 1212.

24. JOLLY, Jacques; TOUZEAU, Michel. Measurement of metastable-state densities by self-absorption technique. *Journal of Quantitative Spectroscopy and Radiative Transfer*. 1975, vol. 15, no. 9, pp. 863–872.
25. SCHULZE, Martin; YANGUAS-GIL, Angel; VON KEUDELL, Achim; AWAKOWICZ, Peter. A robust method to measure metastable and resonant state densities from emission spectra in argon and argon-diluted low pressure plasmas. *Journal of Physics D: Applied Physics*. 2008, vol. 41, no. 6, p. 065206.
26. BOFFARD, John B; JUNG, RO; LIN, Chun C; WENDT, AE. Measurement of metastable and resonance level densities in rare-gas plasmas by optical emission spectroscopy. *Plasma Sources Science and Technology*. 2009, vol. 18, no. 3, p. 035017.
27. NAVRÁTIL, Zdeněk; DOSOUDILOVÁ, Lenka; HNILICA, Jaroslav; BOGDANOV, Todor. Optical diagnostics of a surface-wave-sustained neon plasma by collisional–radiative modelling and a self-absorption method. *Journal of Physics D: Applied Physics*. 2013, vol. 46, no. 29, p. 295204.
28. KRAMIDA, Alexander; RALCHENKO, Yuri; READER, Joseph; TEAM, NIST ASD. *NIST Atomic Spectra Database (version 5.9)*. 2021. Available also from: <https://physics.nist.gov/asd>.
29. GAILLARD, M; BRITUN, Nikolay; KIM, Yong M; HAN, Jeon G. Titanium density analysed by optical absorption and emission spectroscopy in a dc magnetron discharge. *Journal of Physics D: Applied Physics*. 2007, vol. 40, no. 3, p. 809.
30. SAMUELSSON, Mattias; LUNDIN, Daniel; JENSEN, Jens; RAA-DU, Michael A; GUDMUNDSSON, Jon Tomas; HELMERSSON, Ulf. On the film density using high power impulse magnetron sputtering. *Surface and Coatings Technology*. 2010, vol. 205, no. 2, pp. 591–596.
31. BARKER, Paul Michael; LEWIN, Erik; PATSCHEIDER, Jörg. Modified high power impulse magnetron sputtering process for increased deposition rate of titanium. *Journal of Vacuum Science & Technology A: Vacuum, Surfaces, and Films*. 2013, vol. 31, no. 6, p. 060604.

32. ANTONIN, Olivier; TIRON, Vasile; COSTIN, Claudiu; POPA, Gheorghe; MINEA, Tiberiu. On the HiPIMS benefits of multi-pulse operating mode. *Journal of Physics D: Applied Physics*. 2014, vol. 48, no. 1, p. 015202.
33. BARKER, Paul Michael; KONSTANTINIDIS, Stephanos; LEWIN, Erik; BRITUN, Nikolay; PATSCHEIDER, Jörg. An investigation of c-HiPIMS discharges during titanium deposition. *Surface and Coatings Technology*. 2014, vol. 258, pp. 631–638.
34. SOUČEK, Pavel; HNILICA, Jaroslav; KLEIN, Peter; FEKETE, Matej; VAŠINA, Petr. Microstructure of titanium coatings controlled by pulse sequence in multipulse HiPIMS. *Surface and Coatings Technology*. 2021, vol. 423, p. 127624.
35. RAADU, Michael A; AXNÄS, Ingvar; GUDMUNDSSON, Jon Tomas; HUO, Chunqing; BRENNING, Nils. An ionization region model for high-power impulse magnetron sputtering discharges. *Plasma Sources Science and Technology*. 2011, vol. 20, no. 6, p. 065007.

Author's publications not discussed in this work

- **HNILICA, Jaroslav**; KLEIN, Peter; VAŠINA, Petr; SNYDERS, Rony; BRITUN, Nikolay. Dynamics of sputtered particles in multipulse HiPIMS discharge. *Plasma Sources Sci. Technol.* 2023, 32, 045003.
- ŠLAPANSKÁ, Marta; KROKER, Michael; KLEIN, Peter; **HNILICA, Jaroslav**; VAŠINA, Petr. Spatially resolved study of spokes in reactive HiPIMS discharge. *Plasma Sources Sci. Technol.* 2022, 31, 055010.
- ŠLAPANSKÁ, Marta; KROKER, Michael; **HNILICA, Jaroslav**; KLEIN, Peter; VAŠINA, Petr. Single-shot spatial-resolved optical emission spectroscopy of argon and titanium species within the spoke. *J. Phys. D: Appl. Phys.* 2022, 55, 035205.
- SOUČEK, Pavel; **HNILICA, Jaroslav**; KLEIN, Peter; FEKETE, Matej; VAŠINA, Petr. Microstructure of titanium coatings controlled by pulse sequence in multipulse HiPIMS. *Surf. Coat. Technol.* 2021, 423, 127624.
- KLEIN, Peter; **HNILICA, Jaroslav**; FEKETE, Matej; ŠLAPANSKÁ, Marta; VAŠINA, Petr. Spoke behaviour in reactive HiPIMS. *Plasma Sources Sci. Technol.* 2021, 30, 055016.
- BERNÁTOVÁ, Katarína; KLEIN, Peter; **HNILICA, Jaroslav**; VAŠINA, Petr. Temporal studies of titanium ionised density fraction in reactive HiPIMS with nitrogen admixture. *Plasma Sources Sci. Technol.* 2021, 30, 125002.
- BRITUN, Nikolay; **HNILICA, Jaroslav**. Optical spectroscopy for sputtering process characterization. *J. Appl. Phys.* 2020, 127, 211101.
- ŠLAPANSKÁ, Marta; HECIMOVIC, Ante; GUDMUNDSSON, Jon Tomas; **HNILICA, Jaroslav**; BREILMANN, Wolfgang; VAŠINA, Petr; VON KEUDELL, Achim; Study of the transition from self-organised to homogeneous plasma distribution in chromium HiPIMS discharge. *J. Phys. D: Appl. Phys.* 2020, 53, 155201.

- BERNÁTOVÁ, Katarína; FEKETE, Matej; KLEIN, Peter; **HNILICA, Jaroslav**; VAŠINA, Petr. Ionisation fractions of sputtered titanium species at target and substrate region in HiPIMS. *Plasma Sources Sci. Technol.* 2020, 29, 055010.
- FEKETE, Matej; BERNÁTOVÁ, Katarína; KLEIN, Peter; **HNILICA, Jaroslav**; VAŠINA, Petr. Influence of sputtered species ionisation on the hysteresis behaviour of reactive HiPIMS with oxygen admixture. *Plasma Sources Sci. Technol.* 2020, 29, 025027.
- FEKETE, Matej; BERNÁTOVÁ, Katarína; KLEIN, Peter; **HNILICA, Jaroslav**; VAŠINA, Petr. Evolution of discharge parameters and sputtered species ionization in reactive HiPIMS with oxygen, nitrogen and acetylene. *Plasma Sources Sci. Technol.* 2019, 28, 025011.
- SOUČEK, Pavel; DANIEL, Josef; **HNILICA, Jaroslav**; BERNÁTOVÁ, Katarína; ZÁBRANSKÝ, Lukáš; BURŠÍKOVÁ, Vilma; STUPAVSKÁ, Monika; VAŠINA, Petr. Superhard nanocomposite nc-TiC/a-C:H coatings: The effect of HiPIMS on coating microstructure and mechanical properties. *Surf. Coat. Technol.* 2017, 311, 257–267.
- FALTÝNEK, Jan; **HNILICA, Jaroslav**; KUDRLE, Vít. Electron density in amplitude modulated microwave atmospheric plasma jet as determined from microwave interferometry and emission spectroscopy. *Plasma Sources Sci. Technol.* 2017, 26, 015010.
- VORÁČ, Jan; SYNEK, Petr; POTOČŇÁKOVÁ, Lucia; **HNILICA, Jaroslav**; KUDRLE, Vít. Batch processing of overlapping molecular spectra as a tool for spatio-temporal diagnostics of power modulated microwave plasma jet. *Plasma Sources Sci. Technol.* 2017, 26, 025010.
- VORÁČ, Jan; POTOČŇÁKOVÁ, Lucia; SYNEK, Petr; **HNILICA, Jaroslav**; KUDRLE, Vít. Gas mixing enhanced by power modulations in atmospheric pressure microwave plasma jet. *Plasma Sources Sci. Technol.* 2016, 26, 025010.
- SCHÄFER, Jan; **HNILICA, Jaroslav**; ŠPERKA, Jiří; QUADE, Antje; KUDRLE, Vít; FOEST, Rüdiger; VODÁK, Jiří; ZAJÍČKOVÁ,

Lenka. Tetrakis(trimethylsilyloxy)silane for nanostructured SiO₂-like films deposited by PECVD at atmospheric pressure. *Surf. Coat. Technol.* 2016, 295, 112–118.

- **HNILICA, Jaroslav**; POTOČNÁKOVÁ, Lucia; KUDRLE, Vít. Time resolved optical emission spectroscopy in power modulated atmospheric pressure plasma jet. *Open Chemistry* 2015, 13, 577–585.
- POTOČNÁKOVÁ, Lucia; **HNILICA, Jaroslav**; KUDRLE, Vít. Spatially resolved spectroscopy of an atmospheric pressure microwave plasma jet used for surface treatment. *Open Chemistry* 2015, 13, 541–548.
- VORÁČ, Jan; **HNILICA, Jaroslav**; KUDRLE, Vít; DVOŘÁK, Pavel; Spatially resolved measurement of hydroxyl (OH) radical concentration in a microwave plasma jet by planar laser-induced fluorescence. *Open Chemistry* 2015, 13, 193–197.
- PAVLIŇÁK, David; **HNILICA, Jaroslav**; QUADE, Antje; SCHÄFER, Jan; ALBERTI, Milan; KUDRLE, Vít. Functionalisation and pore size control of electrospun PA6 nanofibres using a microwave jet plasma. *Polym. Degrad. Stab.* 2014, 108, 48–55.
- **HNILICA, Jaroslav**; POTOČNÁKOVÁ, Lucia; KUDRLE, Vít. Modulation-induced filament tearing in microwave atmospheric plasma jet. *IEEE Trans. Plasma Sci.* 2014, 42, 2472–2473.
- MANAKHOV, Anton; ZAJÍČKOVÁ, Lenka; ELIÁŠ, Marek; ČECHAL, Jan; POLČÁK, Josef; **HNILICA, Jaroslav**; BITTNEROVÁ, Štěpánka; NEČAS, David. Optimization of cyclopropylamine plasma polymerization toward enhanced layer stability in contact with water. *Plasma Process. Polym.* 2014, 11, 532–544.
- **HNILICA, Jaroslav**; KUDRLE, Vít. Time-resolved study of amplitude modulation effects in surface-wave atmospheric pressure argon plasma jet. *J. Phys. D: Appl. Phys.* 2014, 47, 085204.
- **HNILICA, Jaroslav**; POTOČNÁKOVÁ, Lucia; STUPAVSKÁ, Monika; KUDRLE, Vít. Rapid surface treatment of polyamide 12 by microwave plasma jet. *Appl. Surf. Sci.* 2014, 288, 251–257.

- POTOČŇÁKOVÁ, Lucia; **HNILICA, Jaroslav**; KUDRLE, Vít. Increase of wettability of soft- and hardwoods using microwave plasma. *Int. J. Adhes. Adhes.* 2013, 45, 125—131.
- NAVRÁTIL, Zdeněk; DOSOUDILOVÁ, Lenka; **HNILICA, Jaroslav**; BOGDANOV, Todor. Optical diagnostics of a surface-wave-sustained neon plasma by collisional–radiative modelling and a self-absorption method. *J. Phys. D: Appl. Phys.* 2013, 46, 295204.
- **HNILICA, Jaroslav**; SCHÄFER, Jan; FOEST, Rüdiger; ZAJÍČKOVÁ, Lenka; KUDRLE, Vít. PECVD of nanostructured SiO₂ in a modulated microwave plasma jet at atmospheric pressure. *J. Phys. D: Appl. Phys.* 2013, 46, 335202.
- **HNILICA, Jaroslav**; KUDRLE, Vít; VAŠINA, Petr; SCHÄFER, Jan; AUBRECHT, Vladimír. Characterization of a periodic instability in filamentary surface wave discharge at atmospheric pressure in argon. *J. Phys. D: Appl. Phys.* 2012, 45, 055201.
- **HNILICA, Jaroslav**; POTOČŇÁKOVÁ, Lucia; KUDRLE, Vít. Surface treatment by atmospheric-pressure surfatron jet. *IEEE Trans. Plasma Sci.* 2012, 40, 2925–2930.
- SCHÄFER, Jan; VAŠINA, Petr; **HNILICA, Jaroslav**; FOEST, Rüdiger; KUDRLE, Vít; WELTMANN, Klaus-Dieter. Visualization of revolving modes in RF and MW nonthermal atmospheric pressure plasma jets. *IEEE Trans. Plasma Sci.* 2011, 39, 2350–2351.